Journal of Applied Electrochemistry (2006) 36:557–565
DOI 10.1007/s10800-005-9108-5

The titanium/hydrogen system as the solid-state reference in high-temperature proton conductor-based hydrogen sensors

C. SCHWANDT* and D.J. FRAY
*Department of Materials Science and Metallurgy, University of Cambridge, Cambridge, CB2 3QZ, United Kingdom (*author for correspondence, tel.: +44-1223-334360, fax: +44-1223-334567, e-mail: cs254@cam.ac.uk)*

Received 5 April 2005; accepted in revised form 29 November 2005

Key words: calcium zirconate, hydrogen, proton conductor, reference electrode, sensor, solid electrolyte, titanium

Abstract

It has been demonstrated that a mixture of the solid solutions of hydrogen in α-titanium and β-titanium may be applied as a solid-state hydrogen reference electrode in conjunction with the high-temperature proton-conducting solid electrolyte $CaZr_{0.9}In_{0.1}O_{3-\delta}$. The design and preparation of a sensor that incorporates this type of reference electrode are described, and coulometric titration experiments as well as cell voltage measurements are presented and discussed. The activity of the residual oxygen in the reference material has been identified as a critical parameter that needs to be controlled in order to ensure reliable and reproducible sensor performance. The impact of other impurities in the reference material is also considered.

1. Introduction

Perovskite-type alkaline earth metal cerates and zirconates, partially substituted with a metal sesquioxide, are the most important class of high-temperature proton-conducting solid electrolytes. Well-known examples include $SrCe_{0.95}Yb_{0.05}O_{3-\delta}$, $BaCe_{0.9}Nd_{0.1}O_{3-\delta}$ and $CaZr_{0.9}In_{0.1}O_{3-\delta}$. The materials have been employed as the electrolyte in sensors, fuel cells and steam electrolysers [1, 2].

In a potentiometric hydrogen sensor, the unknown hydrogen activity at the measuring side is compared against the known hydrogen activity at the reference side. The reference standard is most straightforwardly provided by a gas of known hydrogen partial pressure, but the need to rely on continuous supply of gas may complicate design and utilisation of the sensor. The incorporation of a self-contained solid-state reference electrode would be advantageous, but suitable materials are not readily available. Key requirements for a reference material include a thermodynamically fixed activity of the potential-determining species, low polarisability, as well as thermal and chemical stability.

The objective of the present study has been to develop a solid-state reference electrode for hydrogen that may be employed in conjunction with perovskite-type proton conductors at elevated temperatures. Evidently, only metal/hydrogen systems forming two-phase mixtures are applicable. It is considered that the titanium/hydrogen, zirconium/hydrogen and hafnium/hydrogen systems are particularly suitable and the first one of these has been investigated more extensively in this work. Other metal-based systems were disregarded because they are difficult to handle and/or highly reactive, this being true for the alkali and alkaline earth metals as well as the metals of the third subgroup and the rare earth metals. As the high-temperature proton-conducting solid electrolyte, calcium zirconate partially substituted with indium oxide, $CaZr_{0.9}In_{0.1}O_{3-\delta}$, has been selected. Under appropriate conditions, this material exhibits the highest proton conductivity of the calcium zirconate-based electrolytes and a proton transference number of virtually unity. The material also possesses very good mechanical, thermal and chemical stability which renders it superior to the cerates and zirconates of strontium and barium [3–5]. The choice was further encouraged by the fact that $CaZr_{0.9}In_{0.1}O_{3-\delta}$ has already been utilised as the electrolyte in a commercialised sensor [6, 7].

There have been a number of earlier attempts of developing solid-state hydrogen reference electrodes for use in combination with proton-conducting solid electrolytes [8–13]. These will be discussed in context with the results of the present work.

2. Fundamental considerations

2.1. *Defect chemistry, transference properties and conduction domains of* $CaZr_{0.9}In_{0.1}O_{3-\delta}$

Indium substitutes zirconium in the metal sublattice, and charge compensation occurs through the formation of vacancies in the oxygen sublattice.

$$In_2O_3 \xrightarrow{CaZrO_3} 2In'_{Zr} + 3O_O^{\times} + V_O^{\cdot\cdot} \quad (1)$$

Uchida et al. [14, 15] have described the interaction of a proton-conducting oxide-based solid electrolyte with an adjacent phase by three inter-dependent reaction equations, assuming chemical equilibrium between hydrogen, oxygen and water.

$$\frac{1}{2}O_2 + V_O^{\cdot\cdot} = O_O^{\times} + 2h^{\cdot} \quad (2)$$

$$H_2O + 2h^{\cdot} = 2H_i^{\cdot} + \frac{1}{2}O_2 \quad (3)$$

$$O_O^{\times} + 2H_i^{\cdot} = V_O^{\cdot\cdot} + H_2O \quad (4)$$

$$H_2 + \frac{1}{2}O_2 = H_2O \quad (5)$$

Equation (2) describes the exchange of oxygen between the solid electrolyte and the surrounding phase. With increasing occupation of oxide ion vacancies, the concentration of defect electrons rises, so the material is predominantly p-type conducting under oxidising conditions. Equation (3) accounts for the exchange of defect electrons with protons, as it takes place in the presence of water or hydrogen. The protons are associated to oxide ions but sufficiently mobile to render the material proton-conducting at elevated temperatures. Equation (4) is obtained by combination and reflects the exchange of water between the solid electrolyte and the surrounding phase. With increasing temperature, the equilibrium shifts to the right-hand side, causing proton depletion in the electrolyte.

Norby and Kofstad [16] as well as Sutija et al. [17] have derived an equation for the cell voltage, which is established across a proton-conducting oxide-based solid electrolyte in the presence of activity gradients of both hydrogen and oxygen. If it is considered that, apart from protons, H^+, oxide ions, O^{2-}, hydroxide ions, OH^-, and hydroxonium ions, H_3O^+, are potential charge carriers, the general expression for the cell voltage reads as follows.

$$U = \left[t_{O^{2-}} + 2t_{OH^-} - 2t_{H_3O^+}\right]\frac{RT}{4F}\ln\frac{p''_{O_2}}{p'_{O_2}} - \left[t_{H^+} - t_{OH^-} + 3t_{H_3O^+}\right]\frac{RT}{2F}\ln\frac{p''_{H_2}}{p'_{H_2}} \quad (6)$$

where U is the cell voltage, t is the transference number of the respective charge carrier, R is the universal gas constant, T is the absolute temperature, F is the Faraday constant, and p is the partial pressure of the respective gas. The equation turns into the well-known Nernst equation for a hydrogen concentration cell under the condition that the transference number of protons approaches unity.

$$U = -\frac{RT}{2F}\ln\frac{p''_{H_2}}{p'_{H_2}} \quad (7)$$

where the symbols have the same significance as in Equation (6). Accordingly, a proton conductor-based cell functions as a plain hydrogen concentration cell provided the solid electrolyte is a virtually pure proton conductor at both electrodes and thus throughout the entire volume. The oxygen activity gradient contributes to the cell voltage only if an oxygen-containing charge carrier is transferred. This has the advantageous consequence that, in the case of dominating proton conduction, there is no need of explicitly fixing the oxygen activities at the electrodes.

Kurita et al. [18] have determined the locations of the conduction domains of the different charge carriers in the $CaZr_{0.9}In_{0.1}O_{3-\delta}$ solid electrolyte from a series of conductivity measurements at different temperatures and gas atmospheres. The results are reprinted on Figure 1, which shows the conduction domains of protons, oxide ion vacancies and electron holes as a function of the partial pressures of hydrogen and oxygen at elevated temperatures. The conduction domains denote the areas in which the transference numbers of the respective charge carriers are larger than 0.5; whereas the electrolytic domains, i.e., the regions with transference numbers in excess of 0.99, are somewhat narrower. Proton conduction dominates at high

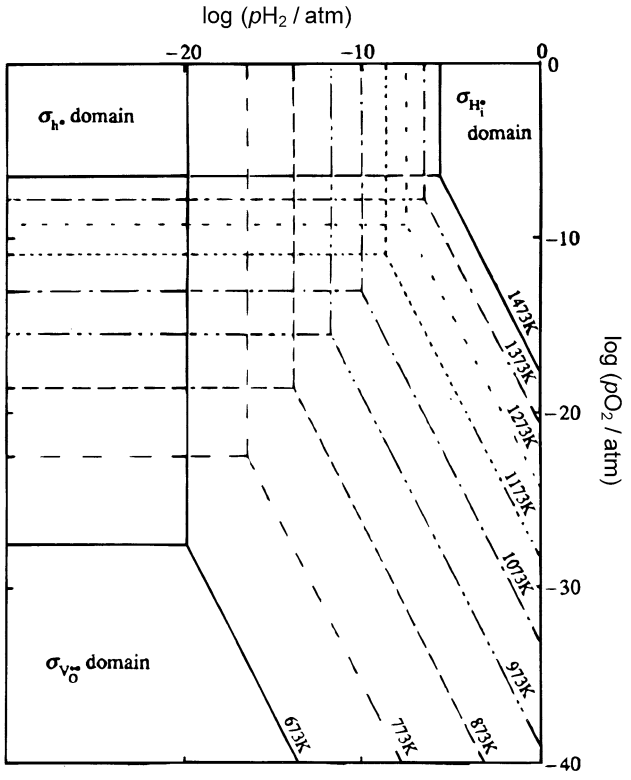

Fig. 1. Conduction domains of the $CaZr_{0.9}In_{0.1}O_{3-\delta}$ solid electrolyte as a function of hydrogen partial pressure and oxygen partial pressure at different temperatures (Reproduced from Reference [18] with permission from The Electrochemical Society).

hydrogen activities but moderate oxygen activities are also required. Low hydrogen and high oxygen activities cause electron hole conduction, while low hydrogen and low oxygen activities give rise to oxide ion vacancy conduction. The domain of electron conduction has not as yet been located. Electron conduction is likely to prevail at extremely low oxygen activities and, although no quantitative information is available, it has been established that the onset of n-type conduction in $CaZr_{0.9}In_{0.1}O_{3-\delta}$ occurs at significantly lower oxygen activities than in calcia-stabilised zirconia [19].

2.2. *Thermodynamic and kinetic properties of the titanium/hydrogen system*

Figure 2 presents the thermodynamic equilibrium phases of the titanium/hydrogen system [20]. In the range of moderate hydrogen contents, there is a two-phase area in which the solid solutions of hydrogen in α-titanium and β-titanium co-exist. The hydrogen partial pressures established over this mixture are in the order of 10^2 to 10^3 Pa at temperatures above 773 K [21]. At higher hydrogen contents, there is another two-phase area and this consists of the solid solution of hydrogen in β-titanium and the δ-phase, i.e., titanium hydride. However, the corresponding hydrogen partial pressures are beyond atmospheric at elevated temperatures [21]. Regarding the kinetic properties of the titanium/hydrogen system, it is known that diffusion of hydrogen in the various solid phases is rapid [22]. The above properties suggest the mixture of hydrided α-titanium and β-titanium for further evaluation.

2.3. *The correlation of electrochemical and thermodynamic aspects*

The interpretation of sensor readings is straightforward only if the sensor may be treated as a hydrogen concentration cell, and the latter demands that the entire solid electrolyte be inside the electrolytic domain of proton conduction. It is evident from Figure 1 that the hydrogen partial pressure generated by a mixture of hydrided α-titanium and β-titanium at elevated temperatures is of a suitable magnitude. As an additional requirement, the oxygen activity must be sufficiently large so that the electrolyte does not fall into the domain of oxide ion vacancy conduction. However, no information exists on the magnitude of the oxygen activity in solid solutions of hydrogen and oxygen in titanium. The only available information correlates the content and the partial pressure of oxygen in the binary titanium/oxygen system and the respective graph is reprinted on Figure 3 [23, 24]. Comparison with Figure 1 reveals that the oxygen activity in such a phase would be too small to permit predominant proton conduction in the solid electrolyte. However, the situation is likely to be different in the ternary titanium/hydrogen/oxygen system as discussed later.

2.4. *The sealing material*

A solid-state reference electrode based on the titanium/hydrogen system must be hermetically sealed. Oxide-based glasses are reliable and easily applicable sealing materials. However, typical solder glasses are silica-based and hence chemically unstable in the presence of high hydrogen partial pressures at elevated temperatures. Other common glass constituents, like the oxides

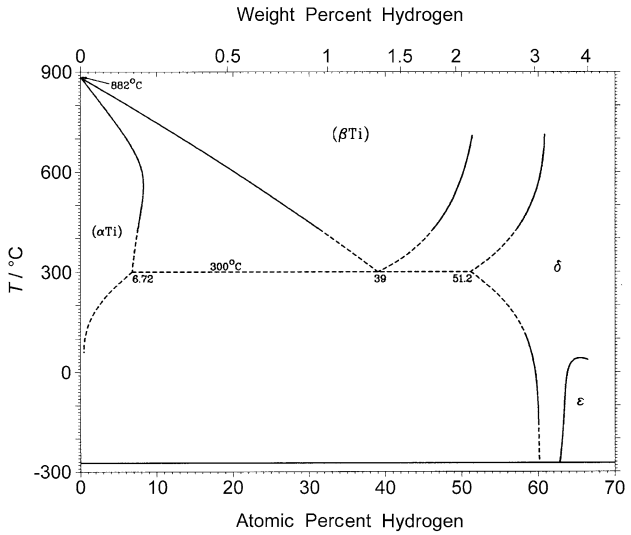

Fig. 2. Phase diagram of the titanium/hydrogen system (Reproduced from Reference [20] with permission from the ASM International).

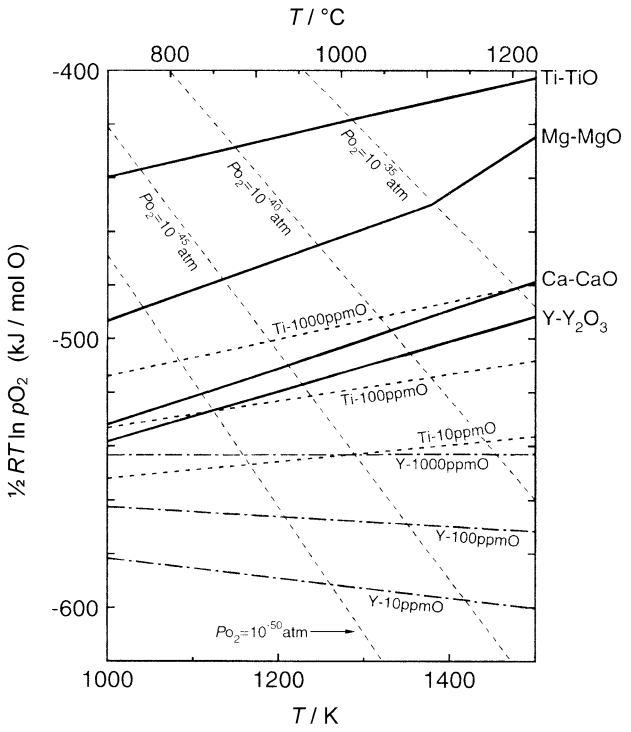

Fig. 3. Partial molar Gibbs free energy and partial pressure of oxygen in the titanium/oxygen binary system at different temperatures in the range of low oxygen contents (Reproduced from Reference [23] with permission from the ASM International).

of sodium, potassium, iron, zinc, lead and phosphorus also have to be avoided. Burggraaf and van Velzen [25] synthesised glasses that consisted exclusively of the oxides of calcium, aluminium, barium, magnesium and boron, and these proved to be stable in the presence of sodium vapour. Näfe [26] developed this type of glass further and prepared glasses of relatively low melting temperatures, reaching approximately 1150 K, and these possessed excellent stability in molten sodium. It is anticipated that this kind of glass is applicable in the presence of hydrogen.

3. Experimental

3.1. *Preparation of the solid electrolyte*

The $CaZr_{0.9}In_{0.1}O_{3-\delta}$ solid electrolyte was prepared via the conventional solid-state chemical route. The required amounts of calcium carbonate, $CaCO_3$, zirconium dioxide, ZrO_2, and indium sesquioxide, In_2O_3, were mixed by ball-milling in propanol-2 for 24 h. The mixed powder was dried and sieved, then calcined at 1573 K in air for 8 h. The calcined material was ball-milled in propanol-2 for 24 h. After drying and sieving, the calcined powder was pressed isostatically at 175 MPa into one-end closed tubes, and these were sintered at 1873 K in air for 8 h. Some of the material was pressed into pellets, sintered under the same conditions, and subjected to X-ray diffraction analysis, density measurements, and proton conductivity measurements.

3.2. *Preparation of the sealing glass*

An oxide glass was synthesised that consisted of 15, 18, 45 and 22 mass% of the oxides of calcium, aluminium, barium and boron, respectively [26]. The required amounts of the oxides or carbonates were mixed, the mixture was calcined and melted in air, held at 1523 K for 10 to 15 min, and then allowed to cool. The solidified melt was ground into a coarse powder. The melting temperature of the glass was approximately 1195 K.

3.3. *Preparation of the sensor*

Porous electrodes at the closed end of the solid electrolyte tube were prepared by covering both surfaces with layers of a platinum-containing ink and annealing at 1273 K in air for 1 h. The coatings were contacted with platinum wires. Typically 40 mg of titanium metal were filled into the electrolyte tube. The remaining volume was packed with calcium zirconate, $CaZrO_3$, powder or yttrium oxide, Y_2O_3, powder. A layer of the sealing glass powder was placed on top. Hydriding of the titanium and formation of the glass seal were performed simultaneously. The assembly was first heated in an alumina tube under an atmosphere of dried and deoxidised pure hydrogen to above the melting temperature of the glass, and then cooled so that the solidifying glass encapsulated the hydrided titanium. Temperature ramps between 5 and 10 K min^{-1} were applied. On heating, a 1–2 h dwell at around 523 K was allowed in order to ensure maximum hydrogen uptake by the titanium. The peak temperature was typically at 1218 K and held for 10 min. During cooling, the rate was reduced to 0.5 K min^{-1} between 1073 and 773 K so as to anneal the solidified glass and avoid the deleterious build-up of mechanical stress. A schematic of the sensor is presented in Figure 4.

The titanium specimen utilised in most of the experiments, and unless stated otherwise, was sheet of commercial purity ASTM 4 (Titanium Metals Corporation; impurity content: oxygen 0.40; nitrogen 0.05; carbon 0.08; iron 0.50; residual elements each 0.10; residual elements in total 0.40; numbers as quoted by the producer in mass%). The sheet was sand-blasted to remove surface impurities, and pieces with surface areas of around 1–2 mm^2 were cut off. In some experiments, titanium sheet of commercial purity ASTM 1 (Titanium Metals Corporation; oxygen content 0.15 mass%) or titanium spheres (William Rowland; oxygen content 0.16 mass%) were employed. The ASTM 1 material was prepared and applied in the same way as the ASTM 4 material. The spheres had diameters between 45 and 500 μm and were used in the as-received state. The oxygen contents of the three materials were confirmed independently and found to agree with the specifications to within 10%. The calcium zirconate or yttrium oxide powders served as chemically inert support for the sealing glass. Pre-investigations had shown that the glass melts and solidifies on top of these materials without undergoing significant compositional changes due to undesired mixing. It was thus possible to prevent direct contact between glass and reference material.

3.4. *Electrochemical measurements*

Coulometric titration experiments were performed at 973 K in a wet mixture of 1 vol% of hydrogen in argon.

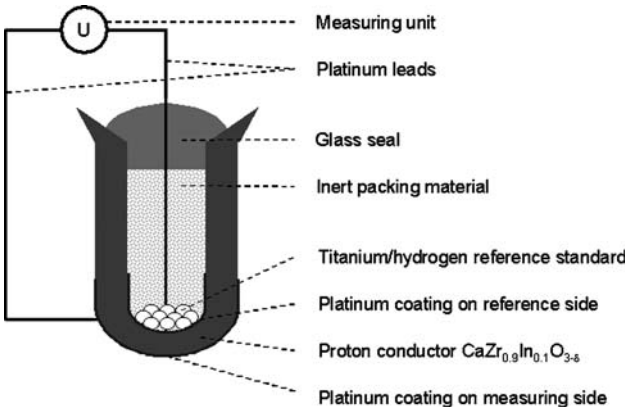

Fig. 4. Schematic of the galvanic cell. The approximate dimensions of the tube are: 20 mm in length, 5 mm outer diameter and 1 mm wall thickness.

Humidification was achieved by passing the gas through water at room temperature, yielding a water vapour content of about 2 vol%. A constant current source was employed, and the currents imposed were usually in the range 20–80 μA. The corresponding applied voltages were mostly no larger than 250 mV, which was well below the decomposition potential of the electrolyte and also precluded excessive electrode polarisation. The titration was interrupted at regular intervals and the cell voltage determined by means of a high-impedance electrometer. In a typical experiment, hydrogen was removed from the reference compartment in steps of 2 C.

In some cases, a coulometric titration experiment was stopped at an intermediate stage and the galvanic cell was subjected to a series of sensor measurements. In these, the cell voltage was recorded while applying temperatures from 773 to 1073 K and hydrogen/argon mixtures with hydrogen contents from 0.01 to 100 vol%. Gas flow rates were between 50 and 200 ml min^{-1}.

4. Results and discussion

4.1. *Properties of the solid electrolyte*

X-ray diffraction analysis of the solid electrolyte material confirmed the overwhelming presence of calcium zirconate, $CaZrO_3$, and also revealed the existence of a minor amount of calcium indate, $CaIn_2O_4$. This was expected, since the solubility limit of indium oxide in calcium zirconate is known to be in the order of approximately 4–5 mol% [3, 5], and shows that the commonly quoted nominal composition of $CaZr_{0.9}In_{0.1}O_{3-\delta}$ is an approximation. The reason for applying a surplus of indium oxide is the empirical finding that this improves reproducibility in the preparation of material of good proton conductivity. Measurements of density and proton conductivity yielded results that closely agreed with previous data [3, 5, 18].

4.2. *Coulometric titration experiments*

Figure 5 compiles the results obtained in three nominally identical coulometric titration experiments carried out at a temperature of 973 K and an external hydrogen partial pressure of 1 vol%. As hydrogen is gradually removed from the reference electrode, the cell voltage decreases. It was noticed that after each current interruption a voltage change of a few millivolts occurred which was likely to reflect depolarisation of the electrodes. Consequently, voltage readings were taken after this transient period of typically no more than a few minutes.

It is expedient to present the coulometric titration curves on a diagram of hydrogen partial pressure vs. hydrogen content of the reference material. The hydrogen partial pressure may be calculated from the cell voltage under the assumption that Equation (7) is applicable. The hydrogen content may be determined from the amount of titanium in the reference compartment and the total charge passed in the course of an experiment. As can be seen on Figure 5, 22 titration steps of 2 C each were performed before the titration reproducibly came to an end during the 23rd step. It is thus assumed that approximately 45 C were necessary to complete an experiment, while some uncertainty as to the precise number remains because it was impossible to exactly identify the endpoint. Figure 6 displays the coulometric titration curves on a linear graph of hydrogen partial pressure vs. hydrogen content of the

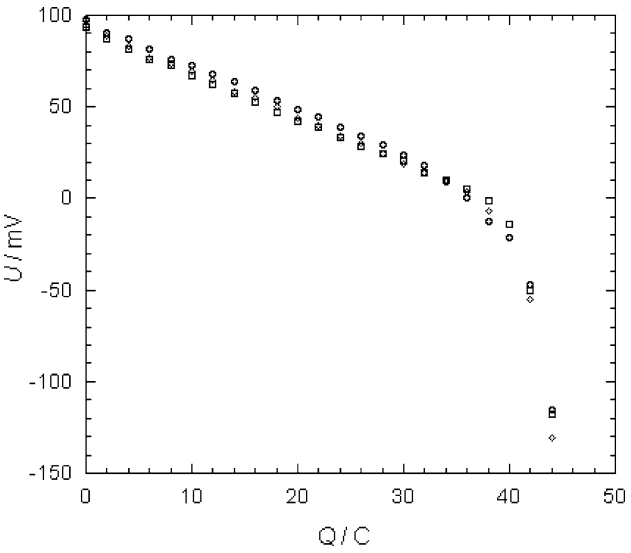

Fig. 5. Coulometric titration curves on a linear diagram of cell voltage vs. charge passed, obtained with 40 mg of hydrided grade 4 titanium metal as the solid-state reference; temperature 973 K, external hydrogen partial pressure 1013 Pa. (The measuring electrode (outer) was connected to the positive terminal, the reference electrode (inner) was connected to the negative terminal.)

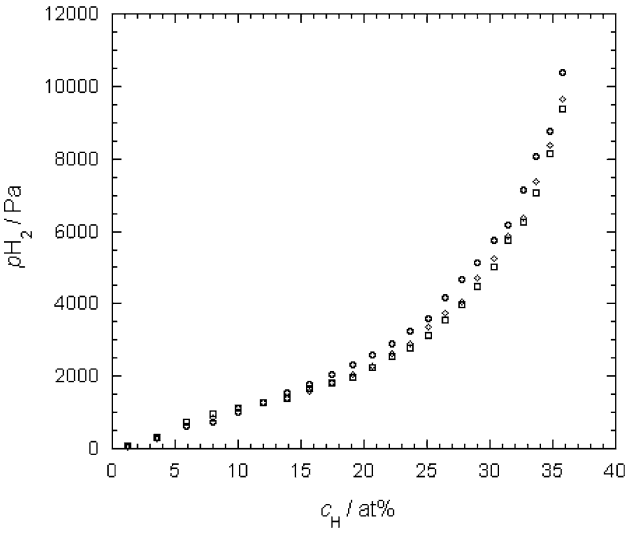

Fig. 6. Coulometric titration curves on a linear diagram of hydrogen partial pressure vs. hydrogen content, obtained with 40 mg of hydrided grade 4 titanium metal as the solid-state reference; temperature 973 K, external hydrogen partial pressure 1013 Pa.

titanium/hydrogen mixture. Commencing from high hydrogen contents, the decline in the hydrogen partial pressure is initially rather steep. In the intermediate region, the pressure falls more slowly, giving rise to a shoulder on the curve. Thereafter, the hydrogen partial pressure decreases somewhat more rapidly again. In the final stage, the pressure approaches zero, indicating that very small hydrogen contents have been reached.

The initial cell voltage, recorded directly after cell preparation, was typically in the range 92–98 mV under the experimental conditions. This voltage is a measure of the amount of hydrogen held by the titanium immediately after formation of the reference material. The value depends crucially on both the hydrogen content of the gas phase and the temperature at which the solidifying sealing glass becomes impervious. In the present case, the initial hydrogen content in the titanium/hydrogen mixture was at approximately 36 mol%.

The most notable feature of the coulometric titration curves is the absence of a genuine hydrogen partial pressure plateau in the titanium/hydrogen composition range where α-titanium and β-titanium are expected to co-exist. The reason lies most probably in the presence of impurities in the titanium specimen employed. Figures 7 and 8 are reprinted from the literature and present double-logarithmic graphs of hydrogen partial pressure vs. hydrogen content for different titanium samples. The diagram on Figure 7 was gained using van Arkel-purified titanium (impurity content: oxygen, nitrogen, carbon, all presumably none; silicon, iron, chromium, magnesium, antimony, copper, in total < 0.07; numbers as quoted in the literature in mass% [27]). Evidently there are almost ideal hydrogen partial pressure plateaux in the two-phase area. The diagram on Figure 8 was obtained with conventional magnesium-reduced titanium (impurity content: oxygen 0.12; nitrogen 0.04; carbon 0.10; silicon 0.04; magnesium 0.13; iron 0.20; manganese 0.02; cobalt 0.02; numbers as quoted in the literature in mass% [28]). Now the relationship between hydrogen partial pressure and composition in the two-phase area is curved and the hydrogen partial pressure for a given composition is shifted to slightly larger values as compared with the ideal case. Both effects were attributed to the presence of impurities in the metal [28]. Figure 9 presents the coulometric titration curves on the same type of graph as those on Figures 7 and 8. Notably, the curves, all of which were recorded at 973 K, coincide almost entirely with the corresponding curve on Figure 8. It is therefore reasonable to assume that the impurity content of the titanium sample utilised was sufficient to cause the specific profile of the coulometric titration curves.

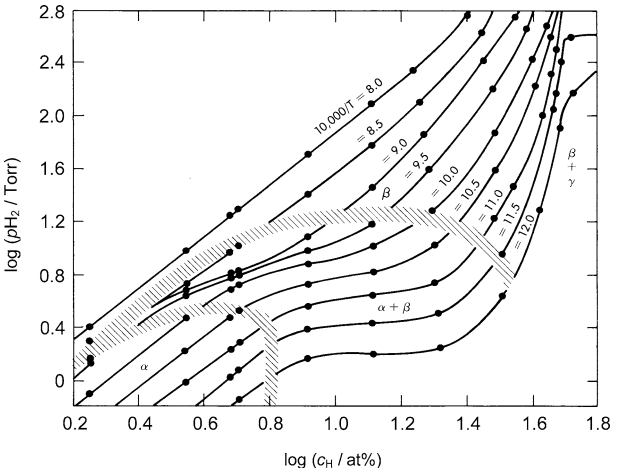

Fig. 8. Double-logarithmic diagram of hydrogen partial pressure vs. hydrogen content for the titanium/hydrogen system at different temperatures, obtained with magnesium-reduced titanium (Reproduced from Reference [21] with permission from Elsevier).

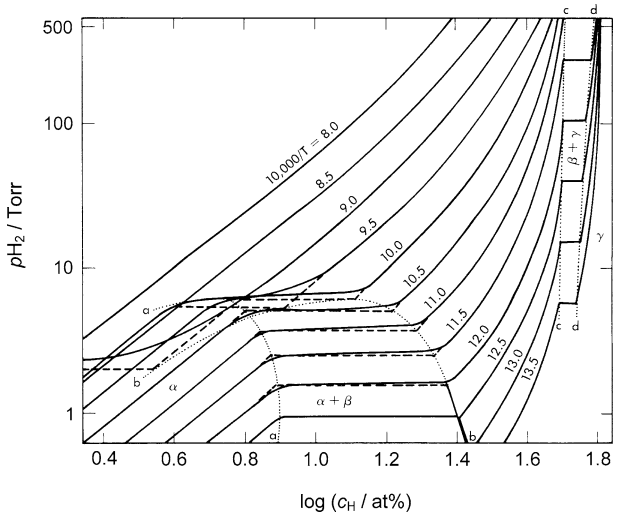

Fig. 7. Double-logarithmic diagram of hydrogen partial pressure vs. hydrogen content for the titanium/hydrogen system at different temperatures, obtained with van Arkel-purified titanium (Reproduced from Reference [21] with permission from Elsevier).

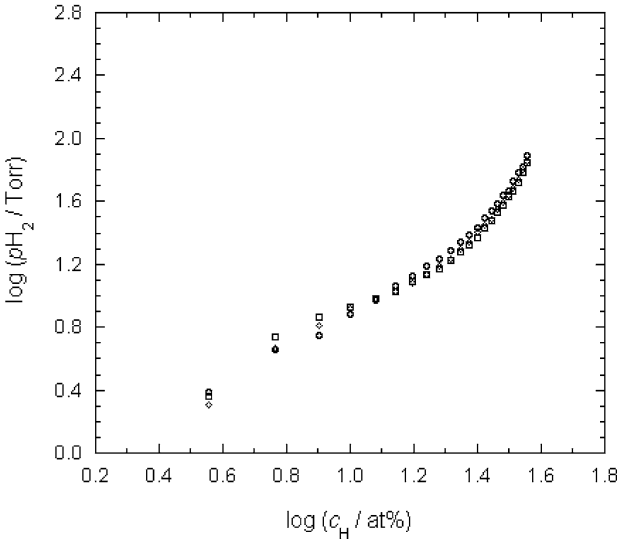

Fig. 9. Coulometric titration curves on a double-logarithmic diagram of hydrogen partial pressure vs. hydrogen content, obtained with 40 mg of hydrided grade 4 titanium metal as the solid-state reference; temperature 973 K, external hydrogen partial pressure 1013 Pa.

4.3. *Cell voltage measurements*

Some of the galvanic cells were subjected to sensor tests. These were performed after interrupting a coulometric titration experiment when a hydrogen partial pressure in the reference compartment of the order of 1400 Pa at 973 K had been reached, which corresponds to a hydrogen content in the titanium/hydrogen mixture of around 14 mol%. The cell voltages, measured for different temperatures and external hydrogen partial pressures, are compiled on Figure 10. The response time to pressure changes was of the order of minutes. Virtually straight lines of Nernstian slope were obtained for all temperatures. Within most of the temperature and hydrogen partial pressure ranges examined, good signal stability was observed, the drift typically not exceeding 0.2 mV h^{-1}. At temperatures above 1073 K and below 773 K, sensor output became progressively unstable. This was, in the former case, probably due to the vanishing of the α-phase and, in the latter case, likely to be associated with the increasing cell impedance. At low temperatures and low hydrogen partial pressures, the flow rate had to be raised to 200 ml min^{-1} in order to attain the expected readings, which suggests sluggish exchange kinetics. The diagram on Figure 10, therefore, covers the appropriate range of operation for the present type of sensor.

The hydrogen partial pressure in the reference compartment is determined by the chemical equilibrium between the two solid phases containing titanium and hydrogen. The exchange of hydrogen between the gas and the solid may be described by the following dissolution reaction.

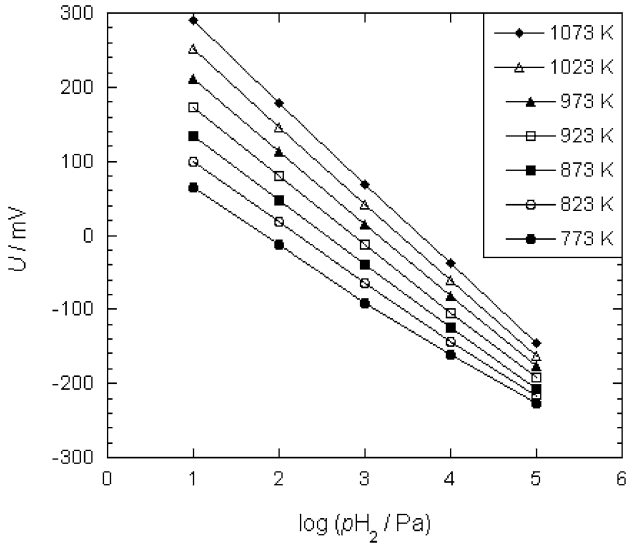

Fig. 10. Cell voltage measurements at different temperatures and external hydrogen partial pressures, obtained with 40 mg of hydrided grade 4 titanium metal as the solid-state reference; internal hydrogen partial pressure, as established through coulometric titration, approximately 1400 Pa at 973 K. (The measuring electrode (outer) was connected to the positive terminal, the reference electrode (inner) was connected to the negative terminal.)

$$H_2(g) = 2H(\text{dissolved in Ti}) \tag{8}$$

The enthalpy of solution of hydrogen in titanium is correlated with the temperature dependence of the hydrogen partial pressure through the van't Hoff equation.

$$R\frac{\mathrm{d}\ln p_{H_2}}{\mathrm{d}(1/T)} = Q \tag{9}$$

where Q is the enthalpy of solution. The hydrogen partial pressure in the reference compartment may be calculated from the cell voltage measured, the temperature, and the external hydrogen partial pressure, provided Equation (7) is valid. As illustrated on Figure 11, evaluation of the experimental data in terms of Equation (9) yields a straight line throughout the entire temperature interval and an enthalpy value of -97 ± 1 kJ mol^{-1}. This number lies between the generally accepted values for solutions of hydrogen in α-titanium, -90 kJ mol^{-1}, and β-titanium, -116 kJ mol^{-1} [21, 27]. This shows that the hydrogen partial pressure in the reference compartment is indeed determined by the equilibrium of α-titanium and β-titanium.

4.4. *Further considerations*

The evaluation of both the coulometric titration experiments and the cell voltage measurements has been carried out under the assumption that the type of galvanic cell employed may be treated as a plain hydrogen concentration cell, and the quality and consistency of the results obtained verify this approach. In fact, more than 20 cells were constructed using grade 4 titanium metal and no irregular behaviour was observed. It may consequently be inferred that the $CaZr_{0.9}In_{0.1}O_{3-\delta}$ solid electrolyte always functioned as a pure proton conductor. The results imply, in view of Figure 1, that the oxygen activity of the solid electrolyte

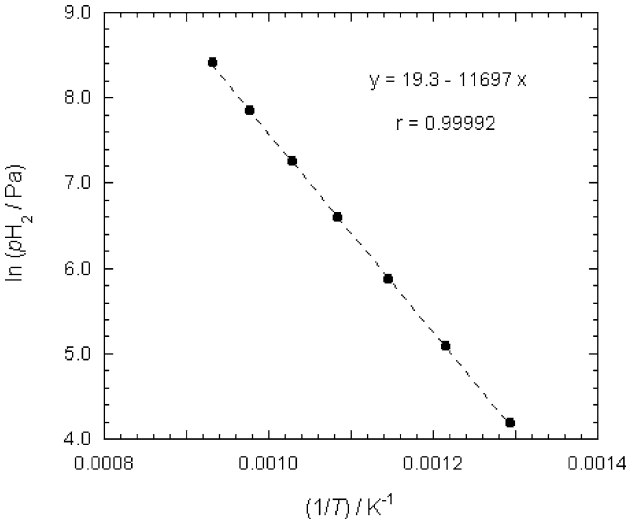

Fig. 11. Natural logarithm of the hydrogen partial pressure of the hydrided grade 4 titanium metal, as determined from cell voltage measurements (cf. Figure 10), vs. reciprocal temperature.

at the interface to the reference electrode must have been larger than 10^{-38} atm at 973 K; this means, in view of Figure 3, that the oxygen activity in the reference material must have been significantly higher than that expected for the binary titanium/oxygen system under otherwise identical conditions.

A rigorous analysis of the empirical findings discussed above is difficult, but a tentative explanation will be given. In terms of the thermodynamics, pure titanium metal is highly reducing and this is manifested in the very low activity of the dissolved residual oxygen. In the reaction with hydrogen, titanium is the more electropositive reactant and so it becomes partially oxidised, its oxidation state assuming a positive value. Accordingly, hydrided titanium is less reducing than pure titanium, hence the oxygen activity in the former is higher than in the latter. A quantitative assessment is impossible due to the lack of data. With regard to the kinetics of the system, titanium metal readily forms an oxygen-enriched surface film. Therefore, if the titanium pieces possess an increased oxygen content at the boundaries, this will lead to enhanced oxygen activity at the interface to the solid electrolyte. Owing to the small diffusion coefficient of oxygen in titanium [29], it may be estimated that this stabilisation remains effective for time periods in excess of the duration of a typical experiment. The above ideas may be corroborated qualitatively through some experimental observations. When replacing the grade 4 titanium metal for grade 1 titanium metal, sensors were mostly found to perform irregularly, exhibiting cell voltages larger than expected and with considerable drift. Probably, the diminished oxygen content in these titanium samples was insufficient to keep the electrolyte within the domain of proton conduction. However, when pre-treating the grade 1 titanium metal with wet hydrogen at elevated temperatures, regular behaviour was again achieved. This suggests the formation of a passivating layer around the titanium particles. The amount of oxygen added must be restricted, for thick layers may inhibit hydrogen permeation and/or the two-component/two-phase approach may be violated. In summary, the experimental results have demonstrated that the activity of the residual oxygen in the titanium/hydrogen system is a critical factor for the performance of the reference electrode. From the practical viewpoint, the suitability of a given titanium variety needs to be assessed experimentally. The same is true when electrolytes other than $CaZr_{0.9}In_{0.1}O_{3-\delta}$ are applied.

4.5. *Discussion of literature*

First attempts of employing a solid-state reference electrode in conjunction with a proton-conducting solid electrolyte were reported by Iwahara et al. [8–10], who proposed the utilisation of solid hydrates like $Ce_2(SO_4)_3 \cdot 8H_2O$ or $AlPO_4 \cdot 0.34H_2O$. These materials determine the water partial pressure rather than the hydrogen partial pressure, but hydrogen sensors based on these reference standards nevertheless provided fair response behaviour under certain conditions. However, signal stability and reproducibility were unsatisfactory and the need of sensor calibration is undesirable. It is probably due to these drawbacks that commercialisation [10] of this type of sensor has not materialised.

The application of a solid metal/hydrogen system in conjunction with a proton-conducting solid electrolyte was reported by Zheng et al. [11–13], who used a Ca/CaH_2 mixture together with the $SrCe_{0.95}Yb_{0.05}O_{3-\delta}$ solid electrolyte. Their hydrogen sensor yielded consistent results for short times but, over a period of hours, the cell voltage drifted markedly. This was ascribed to the thermodynamic instability of the interface of the oxide-based electrolyte and the very strongly reducing reference material. In view of the results from the present study, it is clear that this kind of interface would have to rely on kinetic stability, and stable sensor performance may only be expected at low temperatures.

More recently, and in a different context, Schober [30] has reported the utilisation of the titanium/hydrogen system in combination with a proton-conducting solid electrolyte. Titanium served as a hydrogen storage medium in a proton conductor-based device for coulometric titration of hydrogen into vacuum. In the absence of a current flow, the apparatus could be used as a vacuum leak detector. However, only the qualitative detection of hydrogen in vacuum was described and no attempts of quantitatively analysing hydrogen were communicated.

5. Conclusions

The present study has demonstrated that the solid solution of hydrogen in titanium is capable of serving as a solid-state hydrogen reference electrode in hydrogen sensors, which are based on perovskite-type proton conductors and operated at elevated temperatures. The oxygen activity of the reference material is a parameter of fundamental importance, through which it has to be ensured that the solid electrolyte is inside the electrolytic domain of proton conduction at the interface to the reference electrode. It has been suggested that this may be accomplished either by forming the reference material out of a titanium specimen of a sufficiently high bulk oxygen content, or by passivating the particles of the reference material with an oxygen-rich surface layer. Coulometric titration experiments have revealed that, for hydrided titanium samples of commercial purity, there is no current plateau in the two-phase area of α-titanium and β-titanium but a more s-shaped curve. This is probably due to the presence of impurities in the reference material. Cell voltage measurements yielded results that are in good agreement with thermodynamic data. Reproducibility and stability of sensor output were acceptable.

It is expected that hydrogen sensors that rely on a self-contained solid-state reference electrode will find

important technological applications. One of these is the quantitative determination of hydrogen in molten metals, especially aluminium. Indeed, sensors based on the $CaZr_{0.9}In_{0.1}O_{3-\delta}$ solid electrolyte and the titanium/hydrogen-based reference electrode, or the similar zirconium/hydrogen-based reference electrode, have already demonstrated their potential in numerous successful field trials [31–33].

Acknowledgements

Financial support of this study by the Engineering and Physical Sciences Research Council (EPSRC) of the United Kingdom is gratefully acknowledged.

References

1. H. Iwahara, *Solid State Ionics* **77** (1995) 289.
2. H. Iwahara, *Solid State Ionics* **86–88** (1996) 9.
3. T. Yajima, H. Kazeoka, T. Yogo and H. Iwahara, *Solid State Ionics* **47** (1991) 271.
4. T. Yajima, H. Suzuki, T. Yogo and H. Iwahara, *Solid State Ionics* **51** (1992) 101.
5. H. Iwahara, T. Yajima, T. Hibino, K. Ozaki and H. Suzuki, *Solid State Ionics* **61** (1993) 65.
6. T. Yajima, K. Koide, N. Fukatsu, T. Ohashi and H. Iwahara, *Sensors Actuators B* **13–14** (1993) 697.
7. T. Yajima, K. Koide, H. Takai, N. Fukatsu and H. Iwahara, *Solid State Ionics* **79** (1995) 333.
8. H. Iwahara, H. Uchida, T. Nagano and K. Koide, *Denki Kagaku* **57** (1989) 992.
9. T. Yajima, K. Koide, K. Yamamoto and H. Iwahara, *Denki Kagaku* **58** (1990) 547.
10. T. Yajima, H. Iwahara, K. Koide and K. Yamamoto, *Sensors Actuators B* **5** (1991) 145.
11. M. Zheng and X. Zhen, *Solid State Ionics* **59** (1993) 167.
12. M. Zheng and X. Zhen, *Metall. Mater. Trans. B* **24** (1993) 789.
13. M. Zheng and X. Chen, *Solid State Ionics* **70/71** (1994) 595.
14. H. Uchida, H. Yoshikawa and H. Iwahara, *Solid State Ionics* **34** (1989) 103.
15. H. Uchida, H. Yoshikawa, T. Esaka, S. Ohtsu and H. Iwahara, *Solid State Ionics* **36** (1989) 89.
16. T. Norby and P. Kofstad, *Solid State Ionics* **20** (1986) 169.
17. D.P. Sutija, T. Norby and P. Björnbom, *Solid State Ionics* **77** (1995) 167.
18. N. Kurita, N. Fukatsu, K. Ito and T. Ohashi, *J. Electrochem. Soc.* **142** (1995) 1552.
19. K. Kobayashi, S. Yamaguchi and Y. Iguchi, *Solid State Ionics* **108** (1998) 355.
20. T.B. Massalski (Ed.), *Binary Alloy Phase Diagrams*, 2nd edn., Vol. 2 (ASM International, Materials Park, OH, 1990), p. 2068.
21. W.M. Mueller, J.P. Blackledge and G.G. Libowitz, *Metal Hydrides* (Academic Press, New York, 1968), Chapter 8.
22. H. Mehrer (Ed.), *Landolt-Börnstein, Numerical Data and Functional Relationships in Science and Technology, New Series* (Springer, Berlin, 1990), Group III, Vol. 26, p. 512, 513, 514, 550.
23. T.H. Okabe, T.N. Deura, T. Oishi, K. Ono and D.R. Sadoway, *Metall. Mater. Trans. B* **27** (1996) 841.
24. T.H. Okabe, T.N. Deura, T. Oishi, K. Ono and D.R. Sadoway, *J. Alloys. Comp.* **237** (1996) 150.
25. A.J. Burggraaf and H.C. van Velzen, *J. Am. Ceram. Soc.* **52** (1969) 238.
26. H. Näfe, *J. Nucl. Mater.* **175** (1990) 67.
27. A.D. McQuillan, *Proc. Roy. Soc. (London) Ser. A* **204** (1950) 309.
28. A.D. McQuillan, *J. Inst. Met.* **79** (1951) 371.
29. H. Mehrer (Ed.), *Landolt-Börnstein, Numerical Data and Functional Relationships in Science and Technology, New Series* (Springer, Berlin, 1990), Group III, Vol. 26, p. 476, 487.
30. T. Schober, *Solid State Ionics* **144** (2001) 379.
31. C. Schwandt, D.J. Fray, M.P. Hills, M.A. Henson, R.M. Henson and C. Powell, *Foundry Pract.* **236** (2001) 12.
32. C. Schwandt, D.J. Fray, M.P. Hills, M.A. Henson, R.M. Henson and C. Powell, *Proceedings of the 6th International AFS Conference on Molten Aluminum Processing* (American Foundry Society, Orlando, FL, 2001), p. 148.
33. C. Schwandt, M.P. Hills, M.A. Henson, D.J. Fray, R.M. Henson and A. Moores, *EPD Congress 2003* (The Minerals Metals & Materials Society, San Diego, CA, 2003), p. 427.